UKACC International Conference on Control 2012
Cardiff, UK, 3-5 September 2012

Real Time Estimation of the Wheel-Rail Contact Condtions using Multi-Kalman Filtering and Fuzzy Logic

I Hussain
Mehran University, Jamshoro, Pakistan
imtiaz.hussain@faculty.muet.edu.pk

T. X. Mei
School of Computing, Science and Engineering, University of Salford
T.X.Mei@salford.ac.uk

Mohammad Mirzapour
School of Computing, Science and Engineering, University of Salford
M.Mirzapour@edu.salford.ac.uk

Abstract— **This paper presents a novel technique for the real time estimation of the contact conditions by using a combination of multi-Kalman filtering and fuzzy logic approach. The proposed solution exploits the variations in the dynamic behaviour of a railway wheelset with the changes in wheel-rail contact condition. The proposed system involves the use of multiple model based estimation of the wheelset dynamics in response to different track conditions. Each of the estimators is tuned to match one particular track condition to give the best results at the specific design point. Residuals of each filter are calculated and the level of matches/mismatches is reflected in the residual values of the models concerned. The residuals from all the models are then be assessed by a fuzzy inference system to determine the present operating condition and hence to give real time information about the track conditions.**

Keywords- Wheel rail contact; State Estimation; Kalman filters; Fuzzy Logic

I. INTRODUCTION

Adhesion is a very important factor in the operation of the railway vehicles. The delivery of traction and braking is achieved through the available adhesion at the wheel-rail interface. Insufficient level of adhesion can lead to severe safety and operational problems resulting in huge financial losses to railway industry around the world. Although in last few decades the railway industry is able to manage low adhesion to some extent but currently available measures are not sufficient to eliminate the safety incidents and train delays. This is because the adhesion is affected by a large number of parameters such as weather, season changes and contaminations and therefore cannot be predicted with certainty. Changes in the adhesion conditions can be rapid and also short-lived, and the adhesion coefficient can differ from position to position along a route depending upon the type and degree of contamination which presents a great scientific challenge to effectively design a suitable technique to tackle this problem.

Current wheel slip/slide protection (WSP) technologies for traction and braking systems are incorporated in the rail vehicles to maximize the use of available adhesion [1]. WSPs control the slip ratio (relative speed between a wheel and the train) below a pre-defined threshold to avoid slip/slide during traction or braking [1]. In general, WSPs are effectively reactive systems, i.e. only 'activated' to stop wheel slip/slide when detected by the sensors. There is still a need for a system which is proactive and can prevent slip/slide from its occurrence, such that real time information about the track condition can be provided to the traction and braking control systems to maximize the use of available adhesion. On the other hand, the wheel-rail contact mechanics is extremely complex and vary with time which presents a great scientific challenge to effectively design a suitable technique to tackle this problem.

A number of ideas have been proposed that is related to the monitoring of the running condition of the wheel-rail interface that use low cost inertial sensing mounted on the vehicle and advanced processing, e.g. an inverse modelling approach for the estimation of creep forces [2, 23-25]; and a model based estimation [3-4].

A multiple model approach has been proposed previously by the authors for the real time estimation of the wheel-rail contact conditions [5-8], this paper extends the study to take into account contact conditions that are directly used in design of the Kalman filters. This is of particular practice importance, as real track conditions can be affected by uncertain external factors and hence unpredictable. Furthermore, this paper also covers the complete design of fuzzy inference system and presents a formula to convert the fuzzy logic output into percentage adhesion.

II. MODELLING OF CONTACT MECHANICS

Wheelsets are a key component of railway vehicles that interacts directly with the track and consequently the dynamics of the wheelset are directly influenced by changing contact conditions - therefore this study focusses on a single solid axle wheelset and the outcome of the study may be readily extended to the full vehicles [9-19]. The dynamic behaviour of the railway wheelset is governed by the creep forces generated at the wheel rail contact patches. These creep forces are the result of creepages which are the relative speed of the wheels to rail and can be characterized as lateral (λ_y) and longitudinal creep (λ_x) in accordance with the direction of motion as given in equations 1-3 [5-8].

$$\lambda_{xL} = \frac{r_o\omega_L - v}{v} + [\frac{L_g\dot{\psi}}{v} + \frac{\gamma(y - y_t)}{r_o}] \quad (1)$$

$$\lambda_{xR} = \frac{r_o\omega_R - v}{v} - [\frac{L_g\dot{\psi}}{v} + \frac{\gamma(y - y_t)}{r_o}] \quad (2)$$

$$\lambda_y = \lambda_{yR} = \lambda_{yL} = \frac{\dot{y}}{v} - \psi \tag{3}$$

where the subscripts L and R represent left and right wheels, r_o is the nominal radius of the wheels, v is the vehicle forward speed, γ is the conicity of the wheels, Ψ is the yaw angle, L_g is the track half gauge, ω_L and ω_R are the angular velocities of the left and right wheels respectively, y is the lateral motion, and y_t represents the track irregularity in lateral direction. The total creepage λ_j is the combination of the lateral and longitudinal creepages.

$$\lambda_j = \sqrt{\lambda_{ij}^2 + \lambda_{ij}^2} \quad i = x, y \text{ and } j = L, R \tag{4}$$

The total creep force F_j is a nonlinear function of the total creepage and can be represented using equation 5.

$$F_j = \mu_j N_j \qquad j = L, R \tag{5}$$

The distribution of the contact forces in the longitudinal and lateral directions is thoroughly studied by Polach [20] and can be represented using (6).

$$F_{ij} = F_j \cdot \frac{\lambda_{ij}}{\lambda_j}, \qquad i = x, y \text{ and } j = L, R \tag{6}$$

The equations of motion of the wheelset are given in equations (7-12).

$$M_v \ddot{x} = \frac{\mu_R N_R}{\sqrt{\lambda_{xR}^2 + \lambda_{yL}^2}} \left[\frac{r_o \omega_R - v}{v} - [\frac{L_g \dot{\psi}}{v} + \frac{\gamma(y - y_t)}{r_o}] \right] + \frac{\mu_L N_L}{\sqrt{\lambda_{xL}^2 + \lambda_{yL}^2}} \left[\frac{r_o \omega_L - v}{v} + [\frac{L_g \dot{\psi}}{v} + \frac{\gamma(y - y_t)}{r_o}] \right] \tag{7}$$

$$I_w \ddot{\psi} = \frac{\mu_R N_R}{\sqrt{\lambda_{xR}^2 + \lambda_{yL}^2}} \left[\frac{r_o \omega_R - v}{v} - [\frac{L_g \dot{\psi}}{v} + \frac{\gamma(y - y_t)}{r_o}] \right] L_g - \frac{\mu_L N_L}{\sqrt{\lambda_{xL}^2 + \lambda_{yL}^2}} \left[\frac{r_o \omega_L - v}{v} + [\frac{L_g \dot{\psi}}{v} + \frac{\gamma(y - y_t)}{r_o}] \right] L_g - k_w \psi \tag{8}$$

$$m_w \ddot{y} = -\frac{\mu_L N_L}{\sqrt{\lambda_{xL}^2 + \lambda_{yL}^2}} \left[\frac{\dot{y}}{v} - \psi \right] - \frac{\mu_R N_R}{\sqrt{\lambda_{xR}^2 + \lambda_{yL}^2}} \left[\frac{\dot{y}}{v} - \psi \right] + F_c + F_g \tag{9}$$

$$I_R \dot{\omega}_R = T_t - K_s \theta_s - r_o \frac{\mu_R N_R}{\sqrt{\lambda_{xR}^2 + \lambda_{yL}^2}} [\frac{r_o \omega_R - v}{v} - (\frac{L_g \dot{\psi}}{v} + \frac{\gamma(y - y_t)}{r_o})] \tag{10}$$

$$I_L \dot{\omega}_L = K_s \theta_s - r_o \frac{\mu_L N_L}{\sqrt{\lambda_{xL}^2 + \lambda_{yL}^2}} [\frac{r_o \omega_L - v}{v} + (\frac{L_g \dot{\psi}}{v} + \frac{\gamma(y - y_t)}{r_o})] \tag{11}$$

$$T_s = k_s \int (\omega_R - \omega_L) dt + C_s (\omega_R - \omega_L) \tag{12}$$

where M_v is the mass of the vehicle $\ddot{x}$ is the vehicle forward acceleration, I_w is the yaw moment of inertia, k_w is a yaw stiffness necessary to stabilise the wheelset, m_w is the mass of the wheelset, $\ddot{y}$ is the lateral acceleration, F_c is a centrifugal force which is taken into consideration when the wheelset runs on a curved track, F_g is the gravitational stiffness force related to the lateral displacement and roll angle of the wheelset. The tractive torque T_t is applied to one side of the wheelset (right side in this case) and the other wheel is driven by the torsional torque T_s. $\theta_s = \int(\omega_R - \omega_L) dt$. k_s is the torsional stiffness of the shaft connecting the two wheels and C_s is material damping of the shaft, which is usually very small.

III. Design of Multiple Kalman Filters

The main objective of this study is to detect the changes in the wheel-rail contact condition with practical sensors. The design of the estimator is simplified by considering the wheelset modes that are directly related to contact conditions. Previous studies have suggested that the lateral and yaw dynamics are sufficient for the study of plan-view dynamics of a wheelset [4, 5, 6, 8, 15, 21-22]. The use of a simplified model has several advantages in the estimator design without having a significant effect on the results [5-8]. The major advantage is the simple design of the estimator with minimum number of states which will allow the estimator to converge quickly. The yaw and lateral dynamics are excited by lateral track irregularities. The contact forces given in (5) and (6) are nonlinear in nature and are linearized at specific points on the creep curves in order to enable the design of the Kalman filters. The small signal model of linearized creep forces is given in following equation [5-7].

$$\begin{bmatrix} \Delta\dot{y} \\ \Delta\dot{\psi} \\ \Delta\ddot{y} \\ \Delta\ddot{\psi} \end{bmatrix} = \begin{bmatrix} 0 & 0 & 1 & 0 \\ 0 & 0 & 0 & 1 \\ 0 & \frac{2g_{22}}{m_w} & -\frac{2g_{22}}{vm_w} & 0 \\ -\frac{2L_g \gamma g_{11}}{r_o I_w} & -\frac{k_w}{I_w} & 0 & -\frac{2L_g^2 g_{11}}{vI_w} \end{bmatrix} \begin{bmatrix} \Delta y \\ \Delta\psi \\ \Delta\dot{y} \\ \Delta\dot{\psi} \end{bmatrix} + \begin{bmatrix} 0 \\ 0 \\ 0 \\ \frac{2L_g \gamma g_{11}}{r_o I_w} \end{bmatrix} \Delta y_t \tag{13}$$

The track disturbances (y_t) are very difficult/expensive to measure in practice and therefore highly undesirable to be used as an input to the Kalman filters, therefore (13) is reformulated to include the track input as an additional state, as

$$\frac{d}{dt} \begin{bmatrix} \Delta\psi \\ \Delta\dot{y} \\ \Delta\dot{\psi} \\ \Delta y_t \\ \Delta y - \Delta y_t \end{bmatrix} = \begin{bmatrix} 0 & 0 & 1 & 0 & 0 \\ \frac{2g_{22}}{m_w} & -\frac{2g_{22}}{vm_w} & 0 & 0 & 0 \\ -\frac{k_w}{I_w} & 0 & -\frac{2L_g^2 g_{11}}{vI_w} & 0 & -\frac{2L_g \gamma g_{11}}{r_o I_w} \\ 0 & 0 & 0 & N & 0 \\ 0 & 1 & 0 & 0 & 0 \end{bmatrix} \begin{bmatrix} \Delta\psi \\ \Delta\dot{y} \\ \Delta\dot{\psi} \\ \Delta y_t \\ \Delta y - \Delta y_t \end{bmatrix} + \begin{bmatrix} 0 \\ 0 \\ 0 \\ 1 \\ -1 \end{bmatrix} \dot{y}_t \tag{14}$$

A gyro sensor to measure yaw rate and accelerometer to measure lateral acceleration are found to be sufficient to produce satisfactory results. The output equation is given in (15).

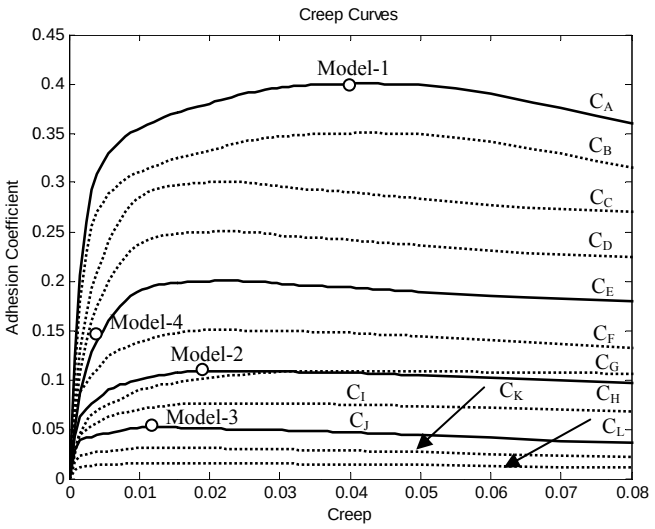

Figure 1. Creep Curves.

$$z(t)=\begin{bmatrix} 0 & 0 & 1 & 0 & 0 \\ \frac{2g_{22}}{m_w} & -\frac{2g_{22}}{vm_w} & 0 & 0 & 0 \end{bmatrix}\begin{bmatrix} \Delta\psi \\ \Delta\dot{y} \\ \Delta\dot{\psi} \\ \Delta y_t \\ \Delta y-\Delta y_t \end{bmatrix}+v \qquad (15)$$

IV. Estimation of Contact Conditions

Several creep curves representing high to very low adhesion conditions are used for the design and the evaluation of the detection system. The creep curves used for the Kalman filter design are shown in solid lines and the creep curves shown in dotted lines are used as additional cases for the assessment of detection system. The proposed scheme is shown in Fig.2. This scheme identifies the contact condition based on the residuals of the Kalman filters, which are the difference generated by the observations and the system's mathematical model. The design of each Kalman filter is based on linerised creep coefficients g_{11} and g_{22} values. At the saturation point of creep curves, g_{11}, which depends upon the slope of the creep curve $d\mu/d\lambda$, is zero and g_{22}, which depends upon traction ratio μ/λ, is different for different adhesion levels. Therefore the residual signal of a Kalman filter designed and tuned to operate in specific contact condition is expected to be at lowest when the vehicle is operated in similar contact condition, in comparison with those from other Kalman filters. In this study, four Kalman filters are found to be sufficient to detect the changes in the contact conditions. Model-1 is tuned to operate at the saturation region of the creep curve C_A, model-2 is designed to operate on the saturation region of the creep curve C_C, model-3 is designed to operate on the saturation region of creep curve C_D and model-4 is designed to operate in the linear region of creep curve C_B. The purpose of the model-4 is to identify whether the wheelset is operating at the saturation region of the creep curve or not.

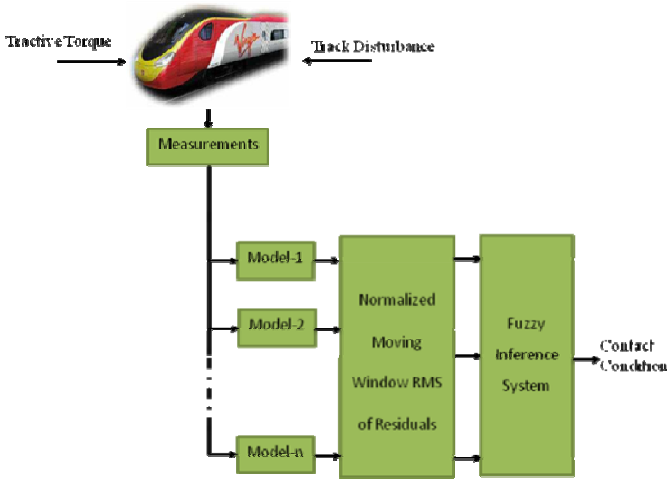

Figure 2. Contact Condition Estimation Scheme

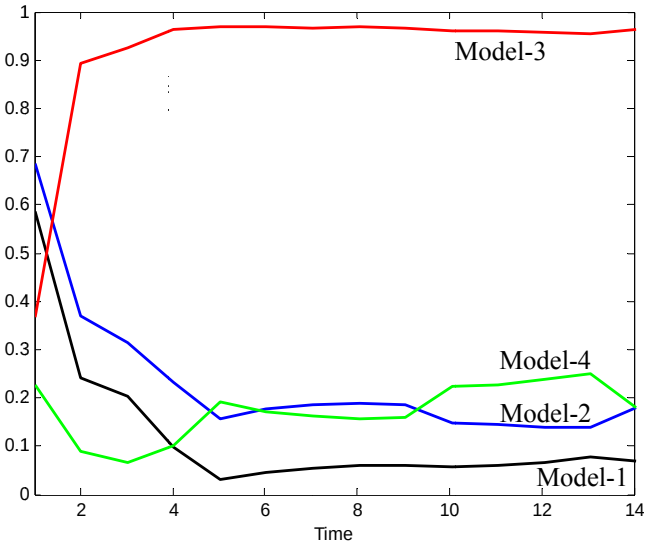

Figure 3. Residuals of filters at P_1

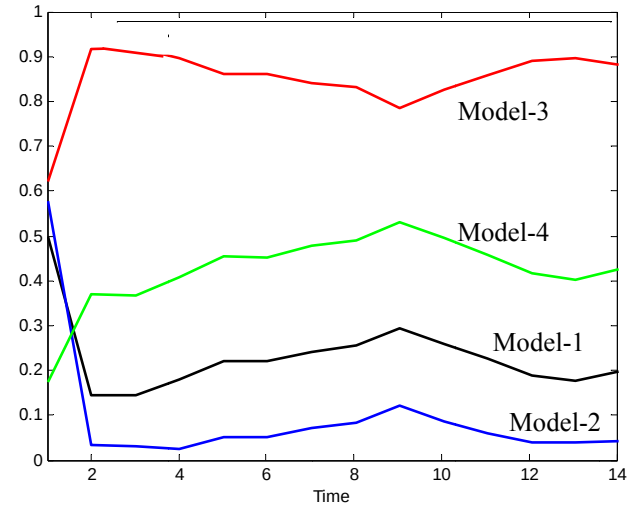

Figure 4. Residuals of filters at P_3

Fig.3 shows the residuals of the filters when the wheelset is operated at the saturation region of the creep curve-1. The

residual of model-1 is the lowest as expected confirming that the wheelset is operating at P_a. When the wheelset is operated at P_c the residual of model-2 is at the lowest and the residual of model-1 is increased as shown in Fig.4. If the wheelset is not operated on the saturation points of the creep curves the residual of model-4 designed at P_e is at the lowest. For instance when the wheelset is operated in the linear region of the creep curve-1 the residual of model-4 is at the lowest as shown in Fig.5.

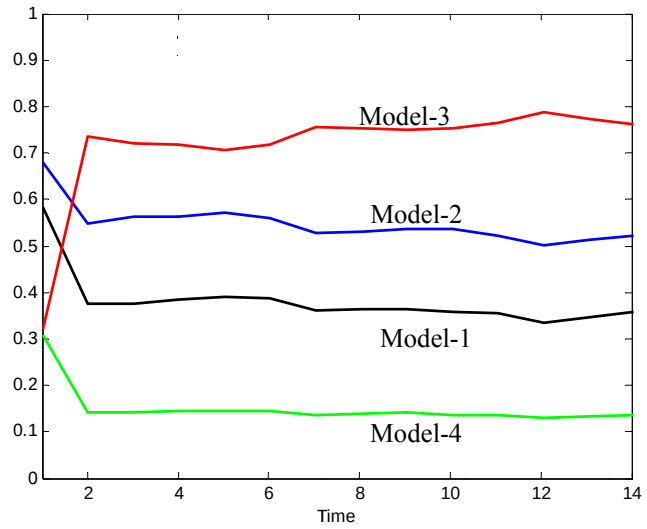

Figure 5. Residuals the when the wheelset is operated in linear region of C_A

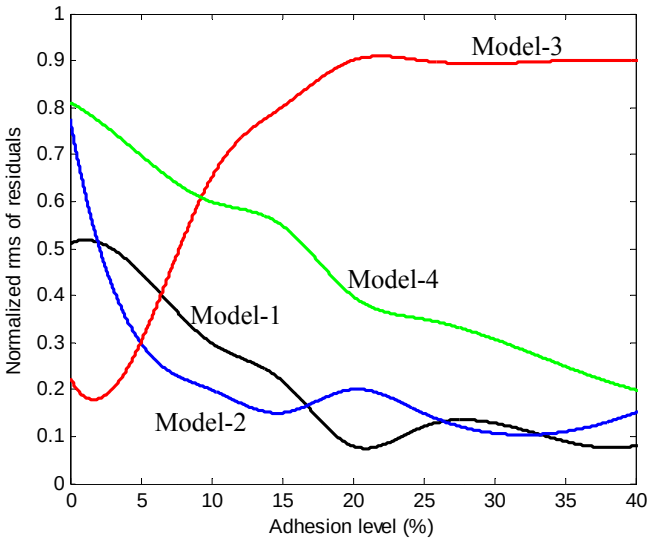

Figure 6. Residuals of filters after interpolation

As only four models are used in the proposed detection scheme, it is necessary to evaluate how the models would respond to other contact conditions that are not directly included in the design. This is carried out by simulating the filters in different contact conditions shown in figure-1 and the residual data is interpolated (Fig.6) to develop a fuzzy logic based detection system to detect other possible contact conditions.

V. Design Of Fuzzy Inference System

The basic idea of the fuzzy inference system is that if wheelset operating point is at the saturation region of the creep curve then the residual information together with the tractive torque can easily be used to determine the adhesion level. The fuzzy inference system (FIS) that analyzes the residuals and the tractive torque is shown in Fig.7. As any other fuzzy logic system it has three main divisions. First part is the input division which scales and weighs the inputs and determines the magnitude of participation in producing output. The inputs are then processed according to set rules and the final output is determined by the averaging the output of individual rules.

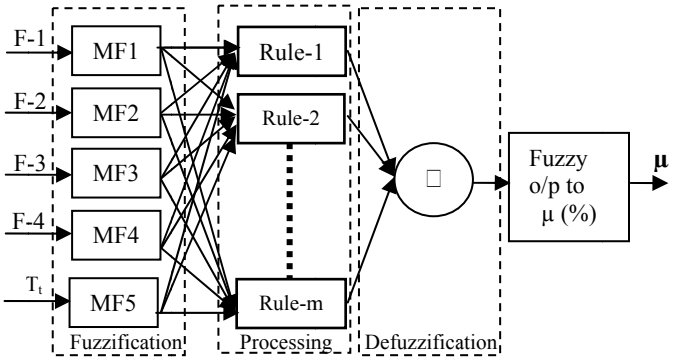

Figure 7. Fuzzy Inference System

The residual of each model in Fig.6 is divided as 'Low', 'Moderate' and 'High' to develop input membership function. Input membership function for residual of model and modle-2 are shown in Fig.8 and Fig.9 respectively.

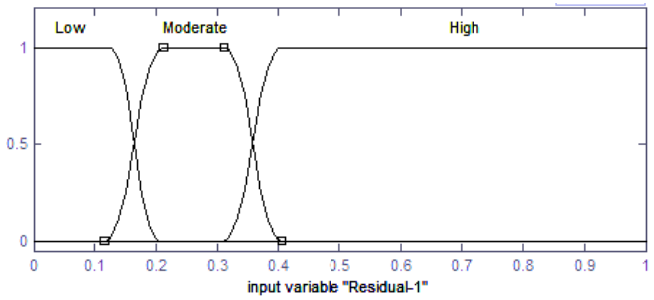

Figure 8. Input membership function of Residual-1

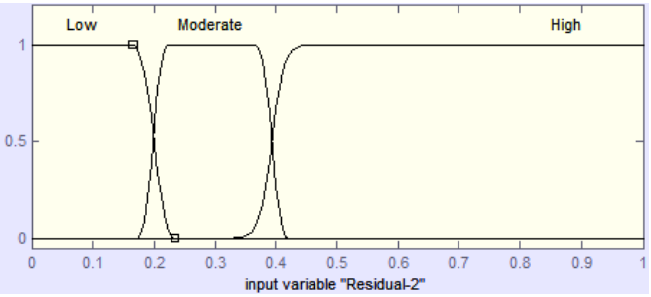

Figure 9. Input membership function of Residual-2

After the residual values are scaled and weighted they are processed according to set rules. The fuzzy logic rules are

developed by examining the residual values in different contact conditions e.g. in 40% adhesion level the value of residual of model-1 is 'Low', the value of residual of Model-2 is 'Low', the value of residual of model-3 is 'High' and the value of residual of model-4 is 'Moderate'. Similarly rules for other possible contact conditions are developed and some of the rules are given below.

If *Residual-1* is '*Low*' and *Residual-2* is '*Low*' and *Residual-3* is '*High*' and *Residual-4* is '*Moderate*' and T_t is 'T_8' then 'μ≥40%'.
If *Residual-1* is '*Low*' and *Residual-2* is '*Low*' and *Residual-3* is '*Moderate*' and *Residual-4* is '*Low*' and T_t is 'T_3' then '20%≥μ≥10%'.

The output is determined by averaging the outcome of all the rules and final numeric output ranging from 0 to 100 is produced. The output fuzzy set is shown in Fig-10.

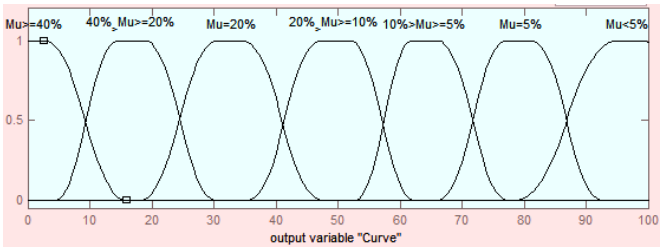

Figure 10. Input membership function of Residual-2

The final stage is to convert the fuzzy logic output into percentage adhesion, which is done by fitting a sixth order polynomial on fuzzy output data set and following equation is obtained.

$$\mu = -2.213\times10^{-6} n_1^{\,4} + 0.00042 n_1^{\,3} - 0.0205 n_1^{\,2} - 0.38 n_1 + 42 \quad (16)$$

where n_1 is fuzzy logic output and μ is percentage adhesion level. The simulations are run different contact conditions and the results are given below.

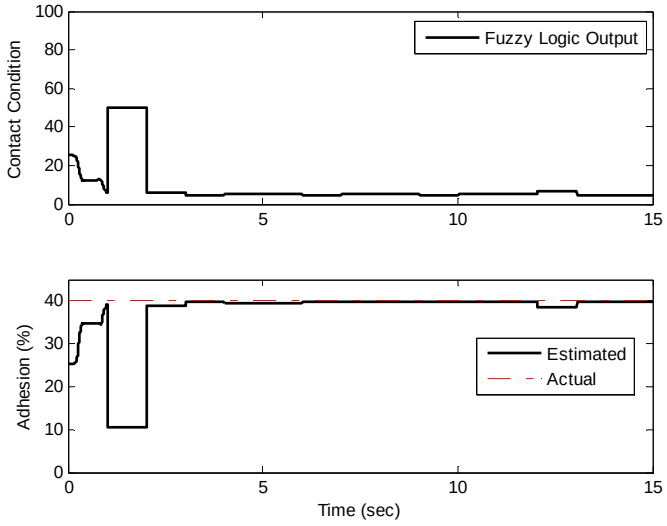

Figure 11. Simulation carried out using creep Curve C_A

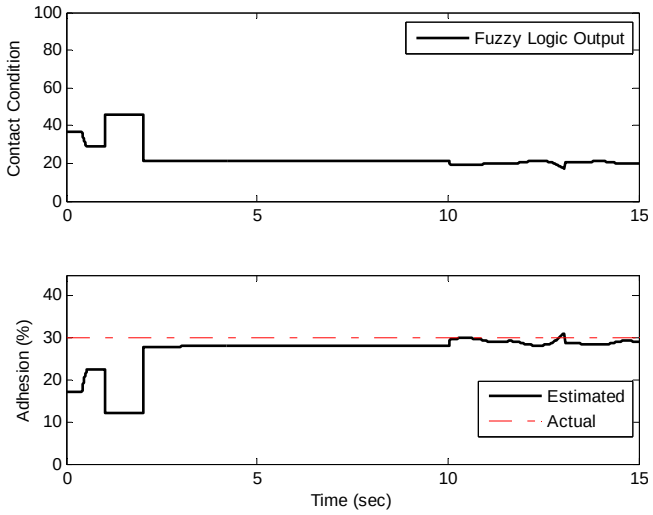

Figure 12. Simulation carried out using creep Curve C_C

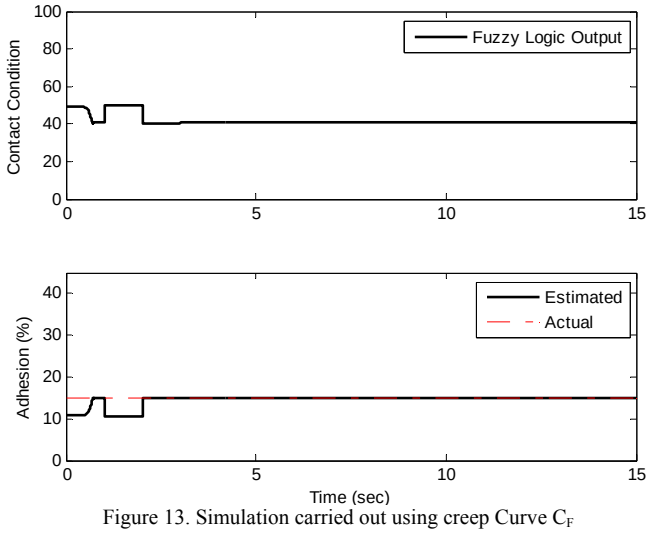

Figure 13. Simulation carried out using creep Curve C_F

Fig.11 shows the output of the fuzzy inference system when the system is operated on creep curve C_A. the fuzzy logic output is converted to adhesion information using (16). The system takes approximately two seconds to react and produce correct output. The delay in this case is due to the time needed in computer simulation to reach steadily contact conditions and also due to the time required to calculate the windowed rms of residuals. After 2 seconds the output fuzzy logic system is steady and the estimated adhesion level is almost equal to the simulated adhesion level. Fig.12 shows the result obtained by simulating the creep curve C_C. Again the steady output is produced after a delay of approximately 2 seconds. In practice while the wheelset already be in motion the amount of delay would not be as much. After the expected delay, the estimated adhesion level is approximately equal to the actual adhesion level. The difference in the actual output and the estimated output is caused by several reasons that include inaccuracy in fuzzy interpretation and the error due to curve fitting formula. Similarly Fig.13 shows the result of the simulation when the wheelset is operated on creep curve C_F.

VI. CONCLUSION AND FURTHER WORK

The problem of low adhesion and its adverse impact on train control systems and rail network operations present a significant technological challenge to the railway industry. Measures taken by railway industries around the world, such as sanding, water jetting, WSPs e.t.c, have solved the problems caused by low adhesion to some extent. But these measures are not sufficient to eliminate the problems completely. The adhesion detection method presented in this paper lays a scientific foundation for a new way forward. The simulation results presented in this paper affirm the potential of the idea presented. Further work, e.g. track testing and experimental validation, will be needed before it can be put into practice.

REFERENCES

[1] Watanabe, T. and A. Yamanaka. "Optimisation of readhesion control of Shinkansen trains with wheel–rail adhesion". Proceedings of the power conversion conferecne, Nagaoka Japan, 1997, p. 47-50.

[2] Xia, F., C. Cole, and P. Wolfs, *An inverse railway wagon model and its applications.* Vehicle System Dynamics, 2007. 45(6): p. 583-605

[3] C. Ward, P.Weston, E. Stewart, H. Li, R. Goodall, C. Roberts, T.X. Mei, G. Charles and R. Dixon, "Condition monitoring opportunities using vehicle based sensors". *IMechE proceedings, Part F: Rail and Rapid Transit*, Vol 225, No.2/2011, pp.202-218.

[4] Charles. G, R. Goodall and R. Dixon. "Model-based condition monitoring at the wheel-rail interface". *Journal of Vehicle System Dynamics*, Volume 46, Supplement 1, pp. 415-430(16), September 2008

[5] Hussain, I. and M.T. X, *Identification of the Wheel Rail Contact Condition for the Traction and Braking Control* Proceedings of the 22nd International Symposium on Dynamics of Vehicles on Roads and Tracks, Manchester Metropolitan University, 14-19 August 2011.

[6] Hussain, M.T.X., *Multi Kalman Filtering Approach for Estimation of Wheel-Rail Contact Conditions* Proceedings of the United kingdom Automatic Control Conferecne 2010, 2010: p. 459-464.

[7] Hussain, M.T.X.a.A.H.J., *Modeling and Estimation of Nonlinear Wheel-rail Contact Mechanics.* Proceedings of the twentieth Intenational conference on System Engineering, 2009: p. 219-223.

[8] Mei, T.X. and I. Hussain. *Detection of wheel-rail conditions for improved traction control*. in *Railway Traction Systems (RTS 2010), IET Conference on*. 2010.

[9] Park. K. T, Lee. H. W, Park. C. H, Kim. D. H and Lee. M. H, "The characteristics of driving control of crane", Proceedings of IEEE International Symposium on Industrial Electronics, Pusan, South Korea, 2001, p. 734 – 739.

[10] Mei, T.X., J.H. Yu, and D.A. Wilson, "A Mechatronic Approach for Anti-slip Control in Railway Traction". Proceedings of the 17th world congress The international federation of automatic control (IFAC), Seoul, Korea, July 2008, p. 8275-8280.

[11] Mei, T.X, J. Yu, and D. Wilson, "A mechatronic approach for effective wheel slip control in railway traction". Proceedings of the Institution of Mechanical Engineers, Part F: Journal of Rail and Rapid Transit, 2009. Vol. 223(3): p. 295-304.

[12] Li. H and R. Goodal, "Modelling and analysis of a railway wheelset for active control", proceedings of the United Kingdom Automatic Control Conferecne, Swansea UK, 1998, p. 1289 – 1293.

[13] Mei, T.X. and R.M. Goodall, "Practical Strategies for Controlling Railway Wheelsets Independently Rotating Wheels". Journal of Dynamic Systems, Measurement, and Control, 2003. Vol. 125(3): p. 354-360.

[14] Yu, J. H, T.X. Mei and D.A. Wilson, "Re-Adhesion control based on wheelset dynamics in railway traction system". Proceedings of the United Kingdom automatic control conferecne, 2006, Sheffield UK.

[15] Yu. J.H, "Re-adhesion control for AC traction system in railway application", PhD thesis, The University of Leeds, 2007.

[16] Iwnicki. S, "Simulation of wheel-rail contact forces". *Journal of Fatigue & Fracture of Engineering Materials & Structures*, vol. 26 No.10, p. 887-900, 2003.

[17] Goodall, R. and H. Li, "Solid Axle and Independently-Rotating Railway Wheelsets-A Control Engineering Assessment of Stability". *International Journal of Vehicle System Dynamics*, Vol.33(1): p. 57-67, 2000.

[18] Goodall, R., "Tilting trains and beyond. The future for active railwaysuspensions. 2. Improving stability and guidance". *Computing & Control Engineering Journal*, 1999. 10(5): p. 221-230.

[19] Beagley, T., I. McEwen, and C. Pritchard, "Wheel/rail adhesion--Boundary lubrication by oily fluids". *Wear*, Vol. 31(1): p. 77-88, 1975.

[20] Polach, O., *Creep forces in simulations of traction vehicles running on adhesion limit.* Wear, 2005. **258**(7-8): p. 992-1000

[21] Charles, G. and R. Goodall. "Low adhesion estimation". IET International Conference on Railway Condition Monitoring, Birmingham, UK, 29-30 Nov. 2006, ISBN: 0 86341 732 9.

[22] Mei, T.X and R. Goodall. "LQG and GA solutions for active steering of railway vehicles". IEEE proceedings on control theory and applications, January 2000, vol. 147(1), p. 111-117.

[23] F. Xia and P. J. Wolfs, "Estimation of wheel rail interaction forces". U.S Patent 7853412 B2, December 2010.

[24] *F.* Xia, S. Bleakley and P. Wolfs, "The estimation of wheel-rail interaction forces from wagon accelerations", Proceedings of the fourth Australasian Congress on Applied Mechanics, Melbourne, Australia, 16-18 February 2005, pp. 333-338

[25] F. Xia and P. J. Wolfs, "Estimation des forces D'Interaction entre des roues et un rail". WO Patent WO/2006/130,908, 2006.